




Article

Anti-Inflammatory Effect of *Pterospartum tridentatum* Leaf Extract in Acute and Chronic Inflammation

Inês Martins Laranjeira ^{1,2,3,4}, João N. D. Gonçalves ⁴, Cátia Gonçalves ⁵ , Marlene Silva ⁶, Nuno Mouta ⁷ ,
Alberto C. P. Dias ⁴ and Filipa Pinto-Ribeiro ^{1,2,*} 

¹ Life and Health Sciences Research Institute (ICVS), School of Medicine, Campus of Gualtar, University of Minho, 4710-057 Braga, Portugal

² ICVS/3B's—PT Government Associate Laboratory, 4710-057 Braga/Guimarães, Portugal

³ CITAB—Centre for the Research and Technology of Agro-Environmental and Biological Sciences, University of Trás-os-Montes e Alto Douro, 5000-801 Vila Real, Portugal

⁴ Centre of Molecular and Environmental Biology (CBMA), University of Minho, Campus de Gualtar, 4710-057 Braga, Portugal

⁵ Department of Biology, University of Aveiro, 3810-193 Aveiro, Portugal

⁶ Instituto Politécnico de Viana do Castelo, 4900-347 Viana do Castelo, Portugal

⁷ Prometheus—Research Unit in Materials, Energy and Environment for Sustainability, Instituto Politécnico de Viana do Castelo, 4900-347 Viana do Castelo, Portugal

* Correspondence: filiparibeiro@med.uminho.pt

Featured Application: *Pterospartum tridentatum* (PtL) is used in popular medicine for its anti-inflammatory properties. Herein, we show PtL extract reversed experimental osteoarthritis induced knee edema, as well as acute ear edema, highlighting its potential as an adjuvant in the management of inflammation.

Abstract: *Pterospartum tridentatum* is an important source of active compounds with anti-inflammatory properties. The ability of *P. tridentatum* leaves methanolic extract in preventing/reversing inflammation was studied in adult rats using a model of experimental osteoarthritis (OA) and ear edema. Control animals (SHAM) were administered phosphate buffer solution (PBS), while OA animals received either *P. tridentatum* 100 mg/kg, 300 mg/kg, or a commercial anti-inflammatory (15 mg/Kg, Ibuprofen) via gavage, daily, for three weeks. Ear edema was induced, and the animals were divided into five groups treated with: (i) ethanol, (ii) *P. tridentatum*, (iii) croton oil, (iv) croton oil + *P. tridentatum*, and (v) croton oil + medrol. The inflammatory effect was evaluated by the measurement of the knee and ear edema. The chromatographic profile, evaluated by HPLC-DAD, showed numerous phenolic compounds are present. In the docking analysis of these compounds, isoquercetin demonstrated strong molecular interactions for peroxisome proliferator-activated receptor alpha and gamma (PPAR α and PPAR γ , respectively), protein kinase 2 subunit α (CK2 α), and 5-lipoxygenase-activating proteins. Genistein had strong docking binding energies for CK2 α and prostaglandin H (2) synthase-1. Our analysis showed the treatment with *P. tridentatum* extract reversed OA-induced edema in the rat knee, as well as ear edema, highlights this plant as a potential source of compounds that can be used as adjuvants in the management of inflammation.

Keywords: *Pterospartum tridentatum*; medicinal plants; bioactive compounds; acute inflammation; methanolic extracts; phytochemicals; experimental osteoarthritis; rat; hyperalgesia



Citation: Laranjeira, I.M.; Gonçalves, J.N.D.; Gonçalves, C.; Silva, M.; Mouta, N.; Dias, A.C.P.; Pinto-Ribeiro, F. Anti-Inflammatory Effect of *Pterospartum tridentatum* Leaf Extract in Acute and Chronic Inflammation. *Appl. Sci.* **2023**, *13*, 4494. <https://doi.org/10.3390/app13074494>

Academic Editor: Monica Gallo

Received: 18 February 2023

Revised: 27 March 2023

Accepted: 29 March 2023

Published: 1 April 2023



Copyright: © 2023 by the authors. Licensee MDPI, Basel, Switzerland. This article is an open access article distributed under the terms and conditions of the Creative Commons Attribution (CC BY) license (<https://creativecommons.org/licenses/by/4.0/>).

1. Introduction

Inflammation is a protective mechanism of the organism against infection or injury to repair tissue structure and its physiological function, restoring homeostasis [1], and can be divided into acute and chronic inflammation. The acute inflammatory response occurs immediately after injury and comprises both the eradication of the infectious agents and a

repair phase in order to return to homeostasis [1,2]. Non-resolving acute inflammation leads to an increased and persistent inflammatory response, becoming chronic inflammation [2].

Current clinical anti-inflammatory therapies include, amongst others, non-steroidal anti-inflammatory drugs (NSAIDs) and glucocorticoids [3]. However, the pharmacological options available display considerable potential for gastric, cardiovascular, renal, and hepatic adverse effects [4], especially in cases of prolonged usage. Therefore, the interest in alternative therapies with anti-inflammatory effects and proven safety has been increasing.

Medicinal plants present many benefits to human health, which are related to the presence of secondary compounds, namely, flavonoids, terpenes, quinones, catechins, alkaloids, and anthocyanins, which display several advantageous properties, including antioxidant, anti-inflammatory, and anti-carcinogenic effects [5,6]. Although plant-derived products are promising, extensive investigation is necessary in preclinical and clinical settings to demonstrate their utility [6,7].

Pterospartum tridentatum (L.) Willk. (previously known as *Chamaespartum tridentatum* P. Gibbs. And *Genista tridentate* L. Willk), or “prickled broom” or “carqueja” in Portugal, is an endemic Leguminosae (Fabaceae) species of Europe belonging to the subfamily Papilionoideae [8,9]. This is an aromatic plant, commonly used in Portuguese gastronomy, and the leaves are conventionally used as a condiment/spice for seasoning of traditional rice and meat dishes [10].

The use of *Pterospartum tridentatum* in traditional medicine as anti-inflammatory [11,12] and its extracts have been described to possess high levels of flavonoids and phenolic compounds [13,14].

We aimed to assess the effect of *P. tridentatum* extracts in acute and chronic inflammation and correlated it with its phytochemical composition. Additionally, we aimed to evaluate the molecular interactions between the major *P. tridentatum* phytochemical compounds and proteins involved in the inflammatory response, thus elucidating its possible mechanism of action.

2. Materials and Methods

2.1. Plant Material

Leaves of *Pterospartum tridentatum* (Figure 1a) were collected in Esposende (41°34'30" N; 8°46'0" W) (Figure 1b), Portugal, in May 2019. The plant material was identified at the Biology Department (University of Minho), and a voucher sample was deposited in the Herbarium of the same Department with the reference 12/2019. The plant material was dried (room temperature) and triturated. The resulting powder was macerated with a methanolic solution (7:3 v/v) (Methanol P.A., Merck) for seven days (100 g of biomass in 1 L of solvent). Subsequently, the solution was filtered and concentrated with a rotary evaporator (Buchi® RII) under reduced pressure (Buchi® V-700 pump, Buchegg, Switzerland) and bath at 50 °C. The extract was lyophilized (Christ® Alpha 2-4, B. Braun, Göttingen, Germany) for two days and stored (dark at room temperature) until further use, following the protocol of Dias and colleagues [15].

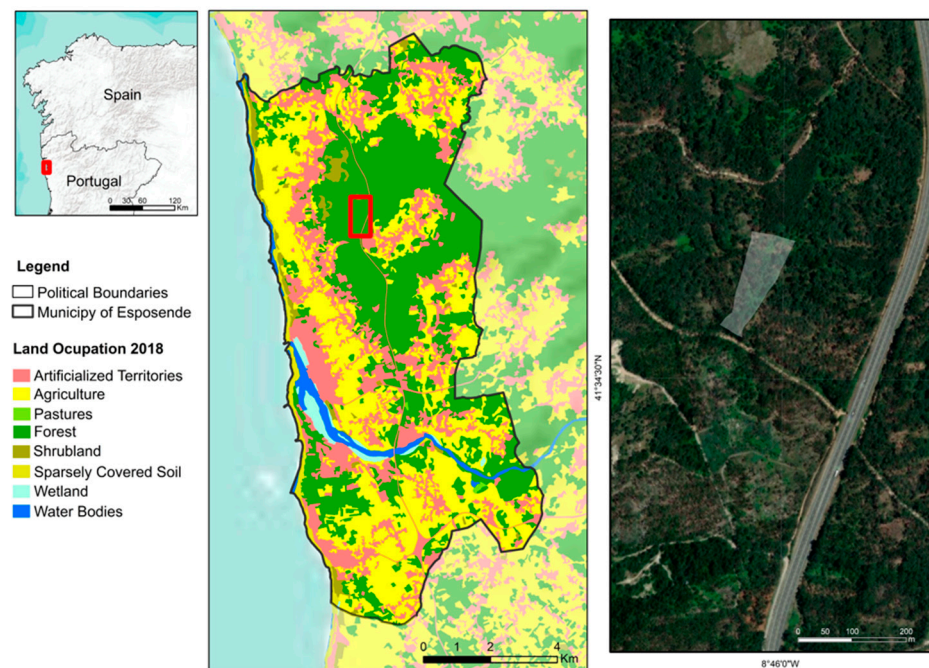
2.2. High-Pressure Liquid Chromatography

HPLC analysis was performed in a Hitachi-Merck HPLC-DAD system (high-performance liquid chromatography with diode array detection), controlled by Merck pc-software (Merck, New York, NY, USA). *P. tridentatum* extract (3 mg/mL) was dissolved in pure methanol and filtered through a 0.2 µm nylon syringe filter (Sigma, Barcelona, Spain). The injection volume was 20 µL.

The solvent system was a gradient based of methanol (HPLC grade, Merck, Darmstadt, Germany) with 0.1% of formic acid (P.A. grade, Merck, Germany) (solvent A) and ultra-pure water with 0.1% of formic acid (solvent B). The optimal elution profile consisted of a six-step gradient: starting with 15% of solvent A and installing a gradient to obtain 15% A at 3 min, 90% (solvent A) at 35 min, 90% (solvent A) at 45 min, 15% (solvent A) at 50 min, and 15% (solvent A) at 60 min.



(a)



(b)

Figure 1. *P. tridentatum* collected specimen (a) and spatial representation of the *P. tridentatum* collection area (area inside red box or area highlighted) (b).

The detection used a diode array detector. Spectral data from all peaks were accumulated in the wavelength range 245–530 nm, and chromatograms were recorded at 260, 280, and 350 nm.

The UV-visible spectra and retention times were used to characterize the presence of phenolic compounds in the samples compared to commercial standard reference compounds, according to Dias and colleagues [15]. The commercial standards (minimum 98% purity) used were taxifolin, rutin, isoquercetin, quercetin, genistin, and genistein, all from Sigma-Aldrich (Barcelona, Spain). The compounds in the chromatogram were quantified by the external standard method. Isoflavone and quercetin derivatives were quantified as genistein and quercetin equivalents, respectively.

2.3. In Vivo Experiments

2.3.1. Ethical Considerations and Handling

The experimental protocol was approved by the Institutional and National Ethical Commission (DGAV 23875/2019) and followed the European Community Council Directive 2010/63/EU concerning the use of animals for scientific purposes. All efforts were made to minimize animal suffering and to use only the number of animals necessary to produce reliable scientific data.

Male Wistar Han outbred *Rattus norvegicus* (Charles Rivers, Barcelona, Spain) weighing between 313–358 g were kept in a controlled temperature environment, mean temperature 22 °C, 55% relative humidity, 12 h light/dark cycle (light cycle starting at 08:00 AM), in standard polycarbonate cages (45.4 cm × 25.5 cm × 20 cm), two animals per cage, with access to water and food (F0021; BioServ, Flemington, NJ, USA) *ad libidum*.

The general health parameters were evaluated weekly. Initially, animals were handled daily by the researcher for 15 days. All subsequent protocols were performed during the day (light phase). When possible, the experimenters were blind to the experiment.

2.3.2. Induction of Ear Oedema

Acute dermal irritation of rat ears was induced using croton oil, 6 h before euthanasia, with a methodology similar to Rodrigues et al. [16], but this involved switching from acetone to ethanol as the vehicle due to the latter presenting superior solubility of the extract.

For this experiment, 26 animals were first divided in two groups: (1) a control group, to which 20 µL of pure ethanol (ETOH) was administered to the inner surface of the ear tip; and (2) an acute inflammation group (CO), to which 20 µL of a fresh solution of croton oil 5% was administered to the inner surface of the ear tip. Fifteen minutes later, the groups were subdivided into: (1) controls receiving a second dose of 20 µL of pure ethanol (ETOH-ETOH, $n = 5$); (2) controls receiving 20 µL of *P. tridentatum* extract dissolved in ethanol (100 mg/mL) (ETOH + PtL, $n = 5$), and the acute inflammation group was treated with either (3) 20 µL of pure ethanol (CO-ETOH, $n = 5$), (4) 20 µL of *P. tridentatum* extract dissolved in ethanol (100 mg/mL) (CO + PtL, $n = 6$), or (5) 20 µL of Medrol dissolved in ethanol (1 mg/mL of active principle; Medrol, Sigma, Portugal) (CO + ME, $n = 5$).

2.3.3. Macroscopic Assessment of Ear Oedema

Ear oedema was calculated as ear thickness variation from controls, measured using a micrometer (Analog external micrometer, 0 to 25 mm, resolution 0.001 mm, Mitutoyo, Aurora, IL, USA). Ear thickness was measured after 6 h of the second application of the various compounds followed by occlusion.

2.3.4. Histological Processing of Ear Samples

After occlusion, ear biopsies (6 mm diameter) were collected using a metal punch and preserved in 4% paraformaldehyde (PFA) (DAC, Applichem Panreac, ITW Companies, Barcelona, Spain).

Histological processing followed a protocol described by Oliveira et al. [17]. Briefly, each sample was placed in cassettes (Biocassette, Bio Optica, Milano Italy), identified, and placed in 4% PFA (DAC, Applichem Panreac, Barcelona, Spain) at room temperature.

Samples were dehydrated in ascending grade ethanol/water solutions (from 70 to 100%) using an automatic sample processor (Leica AutoStainer XL, Nussloch, Germany) for 19 h followed by washing thrice with xylene (C8H10, Carlo Erba, Val de Reuil Cedex, Dasit Group, France). Afterward, the specimens were immersed in paraffin (Thermo Scientific, Cheshire, UK) at 62 °C and allowed to solidify at −5 °C. Specimens were cut into 4 µm thick sections and mounted on a Superfrost glass slide (25 mm × 75 mm × 1 mm, Superfrost Plus, Thermo Scientific, Cheshire, UK). Before staining, the slides were deparaffinized in an automated slide processing apparatus (Leica AutoStainer XL, Nussloch, Germany), and they were stained with hematoxylin Harris (Millipore Corporation, Massachusetts, MA, USA) for 1 min followed by a bath in tap water for 2 min. Then, slides were washed

with 0.5% of ammonia solution (Sigma Aldrich, Madrid, Spain) for 10 s, washed with tap water for 1 and half minutes, and washed with 96% ethanol solution (45 s). Slides were then immersed in eosin Y solution (Thermo Scientific, Cheshire, UK) for 30 s and dehydrated with 96% ethanol (1 min), absolute ethanol (2 min each time), and xylene (first wash for 1 min and the second for 2 min). Slides were mounted using resinous medium (Entellan, Merck, Darmstadt, Germany), and they were covered with lamellae (24 × 60 mm, Superfrost Plus, Thermo Scientific, Cheshire, UK). Finally, the slides were allowed to air dry for seven days.

2.3.5. Histopathological Assessment of Ear Samples

Histopathological analysis of ears was performed to analyze the existence/absence of acute inflammation after the application of croton oil and the anti-inflammatory effect of *P. tridentatum* extracts. The assessment was based on the thickness of the dermis and epidermis and the presence of inflammatory cells after each treatment.

Measurement of dermis and epidermis thickness was performed using an optical microscope (Olympus BX61, Tokyo, Japan) interconnected to a digital color camera (Olympus, DP70, Tokyo, Japan) through the CellSens Dimension software (Olympus Corporation, Münster, Germany) at 100× amplification. For each ear sample, nine random measurements were made.

Slides were then photographed using the CellSens Dimension Olympus software (Olympus Corporation, Münster, Germany) on an optical microscope (Olympus, BX61) coupled to a digital color camera (Olympus, DP70, Münster, Germany), and the number of inflammatory cells was counted.

2.3.6. Experimental Osteoarthritis (OA) Induction

For the induction of experimental OA, the animals were anesthetized with a mixture of ketamine (0.75 mg/kg, Imalgene, Merial, Oeiras, Portugal) and medetomidine (0.5 mg/kg Dorbene, Esteve, Carnaxide, Portugal).

For the induction of OA [18], a mixture of 0.1 mL of 3% carrageenan 3% kaolin (Sigma-Aldrich, StLouis, MO, USA) dissolved in a sterile saline solution (NaCl 0.9% pH 7.2, Unither, Amiens, France) was injected into the right knee joint with a hypodermic needle (P20, 0.3 mm × 13 mm, Microlance, UK). The animals of the sham group were injected with 0.1 mL of vehicle (NaCl 0.9% pH7.2, Unither, Amiens, France). To guarantee the distribution of the mixture and the start of the degradation of the cartilage, the animal's paw was flexed and extended ten times.

Afterwards, the anesthesia was reversed using atipamezole hydrochloride (1 mg/kg, Antisedan, Pfizer, Oeiras, Portugal, i.p.) according to the protocol of David-Pereira et al. [19]. Animals were observed until eating and grooming, and welfare was evaluated daily (grooming, dehydration/weight loss, and locomotor abnormalities).

2.3.7. Drug Preparation and Administration

Powdered extract of *P. tridentatum* was dissolved in PBS 10 mM (137 mM NaCl, 2.7 mM KCl, 10 mM Na₂HPO₄, 2 mM KH₂PO₄, 1% Tween 20 (Applichem, Panreac, ITW companies, Barcelona, Spain), pH 7.4), placed on an ultrasound bath (Sonicator Branson 2510, Emerson Corporate, London, UK) for 30 min and stored in the dark at room temperature.

The administered concentration of the extract was adjusted weekly according to the animals' body weight to the final concentrations of 100 mg/kg and 300 mg/kg of *P. tridentatum*, respectively. Before administration, the extract solution was sonicated for 15 min.

Administration of the treatment was performed daily for three weeks through gavage. Controls animals were administered the vehicle solution.

2.3.8. Pressure Application Measurement (PAM)

Mechanical hyperalgesia in the knee was evaluated using the pressure PAM method [20]. Briefly, with the animal securely held, an increasing force was gradually applied across the joint of interest until it reached the maximum force required to elicit a response: paw withdrawal, vocalization, or wriggling movements. The results correspond to the force peak applied immediately before the response and are presented in grams force (gf) [21,22].

The measurements were recorded as the limb withdrawal threshold (LWT). LWT was measured twice on each knee joint at 1 min intervals. The mean LWTs were calculated per animal.

2.3.9. Perimeter of Knee

Oedema of the knee joint in rats was evaluated by measuring the perimeter of the right knee in each rat, as described by Adães and colleagues [23]. The measurement was performed at specific times throughout the experiment: (1) before the induction of OA; (2) two weeks after surgery; and (3) after treatment. The measurement was made in the region of the kneecap. The edema results are expressed in centimeters.

2.3.10. Experimental Design

- Experiment 1

To test the effect of PtL extract in acute inflammation, animals were challenged through the application of an irritant, croton oil (CO) applied topically in the ear inner surface. For this purpose, animals were first administered either ethanol (ETOH) or croton oil (CO) followed by treatment 15 min later. Treatment consisted in the application of either vehicle (ETOH), and *P. tridentatum* extract (ETOH + PtL and CO + PtL), or an anti-inflammatory drug (glucocorticoid; CO + Medrol). Assessment of the anti-inflammatory efficacy of treatments was evaluated 6 h later by measuring ear thickness followed by ocision. Ear samples collected through the punch method were preserved in PFA 4%, processed, and histopathologically evaluated.

- Experiment 2

Before the induction of experimental OA, baseline assessments of mechanical hyperalgesia and perimeter of knees were performed in all animals. Animals were allocated to one of two experimental groups, OA ($n = 19$), or SHAM ($n = 4$). SHAM and OA surgeries were performed on the same day, and animals were henceforth re-tested weekly. Two weeks post-OA induction, OA animals were subdivided into four groups to receive administration of either the extract (PtL) at a concentration of either 100 mg/kg (OA_PtL100, $n = 5$), or 300 mg/kg (OA_PtL300, $n = 5$), or PBS 1 mg/kg (OA-VEH, $n = 5$), or a nonsteroidal anti-inflammatory drug (Ibuprofen—Brufen, Mylan, EUA) at 15 mg/kg (OA_AI, $n = 4$), daily, for a period of three weeks. Sham rats received the vehicle (PBS) alone (SHAM_VEH, $n = 4$).

2.4. Computational Models—Molecular Docking

The crystal structure of peroxisome proliferator-activated receptor alpha and gamma (PPAR α (2P54) and PPAR γ (6TSG), respectively), mPGES-1 (4YL1), prostaglandin H (2) Synthase-1 (1Q4G), protein kinase CK2 α (6TGU), inhibitor-bound human 5-lipoxygenase-activating protein (2Q7M), and the crystal structure of mPGES-1 bound to inhibitor (5T36) were obtained from the Protein Data Bank (<https://www.rcsb.org/pdb>, accessed on 8 January 2023). The initial crystal structures were processed with Pymol tools 2.5.2 by removing non-polar water molecules and adding polar hydrogen. The original charges of the crystal structures were saved, and the files were exported as .pdbqt. The three-dimensional structure of isoquercetin, quercetin, and genistein were downloaded from NCBI (<https://pubchem.ncbi.nlm.nih.gov/>, accessed on 8 January 2023), which were then optimized with Pymol 2.5.2 software and processed with AutoDock 4.2 to form .pdbqt files for docking studies.

The probable interaction between bioactive compounds and crystal structures of the mentioned proteins was explored by AutoDock 4.2 with the grid box centered at the protein active center. The docking calculations were performed 250 times runs by the Lamarckian genetic algorithm. The protein–ligand complexations that possess the minimum energy scoring of -7 Kcal/mol were selected for further visualization of the docked conformation with Discovery Studio Software (Biovida Dassault Systèmes, Discovery Studio Software, version 4.5, San Diego, CA, USA). [24].

2.5. Statistical Analysis

Statistics were performed using the GraphPad Prism 5 software (GraphPad Software Inc., version 5, LaJolla, CA, USA). For comparing groups in the acute dermal irritation test a T-test between experimental groups (ETOH and ETOH + PtL; ETOH and ETOH + CO) was performed, followed by a one-way analysis of variance (ANOVA one-way) between the CO group and treatments (ETOH + CO, CO + PtL and CO + Medrol), followed by the Bonferroni post hoc test.

For the analysis of chronic inflammation data (PAM and Knee oedema), a two-way ANOVA was performed, followed by Bonferroni post hoc test. $p < 0.05$ was considered statistically significant.

3. Results

3.1. Identification of Phenolic Compounds by HPLC-DAD

The methanolic powder extract of leaves of *P. tridentatum* was subjected to HPLC-DAD analysis (Figure 2). Phenolic compounds were identified by direct comparison of the chromatogram with commercial standards (Table 1, peaks 14–17 and 22) or based on retention time and UV-Vis absorption spectra (Table 1, peaks 19, 20, 23, 24). Peaks 19, 20, and 24 were identified as isoflavone derivatives based on their UV spectra (λ_{\max} at 260–262 nm) and similarity with genistein spectra. Peak 23 has a spectra similar to quercetin (λ_{\max} at 256, 370 nm), but with a slightly different RT. So, this compound was identified as a quercetin derivative. The identification of these compounds agrees with previous works [14,25]. Taken together, these compounds represent the major phenolics found in our *P. tridentatum* extract.

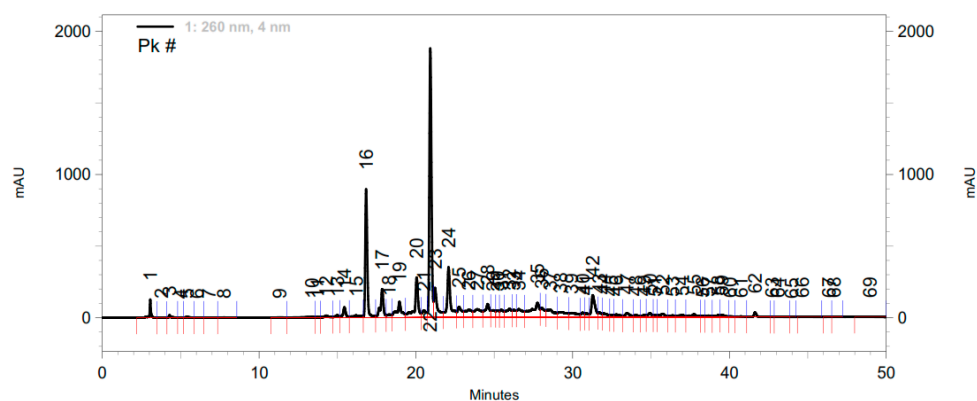


Figure 2. HPLC-DAD-UV (260 nm) phenolic profile of the methanolic extract from leaves of *P. tridentatum*.

3.2. Macroscopic Assessment of Ear Edema

Macroscopic evaluation of ear thickness reveals the application of *P. tridentatum* extract alone (ETOH + PtL) did not alter this parameter when compared to the control group (ETOH) (Figure 3a: $t_{(8)} = 0.4174$, $p = 0.6874$). Croton oil application (CO + ETOH) significantly increased macroscopic ear thickness when compared to the control group (ETOH) (Figure 3a: $t_{(8)} = 11.22$, $p < 0.0001$). Further analysis showed significant differences in macroscopic ear thickness after treatment (Figure 3a: ANOVA_{one-way}: $F_{(2,13)} = 49.60$, $p < 0.0001$),

with post hoc tests demonstrating the application of *P. tridentatum* methanolic extract, and Medrol counteracted ear thickness increase after CO application.

Table 1. Phenolic composition of the *P. tridentatum* extract.

Peak	Retention Time (min)	Compound	µg/mg dwb
14	15.447	taxifolin	12
15	16.186	rutin	8
16	16.827	isoquercetin	135
17	17.853	genistin	33
19	18.953	i.d.	29
20	20.053	i.d.	53
22	20.920	genistein	225
23	21.220	q.d.	52
24	22.087	i.d.	65

i.d.—isoflavone derivative; q.d.—quercetin derivative.

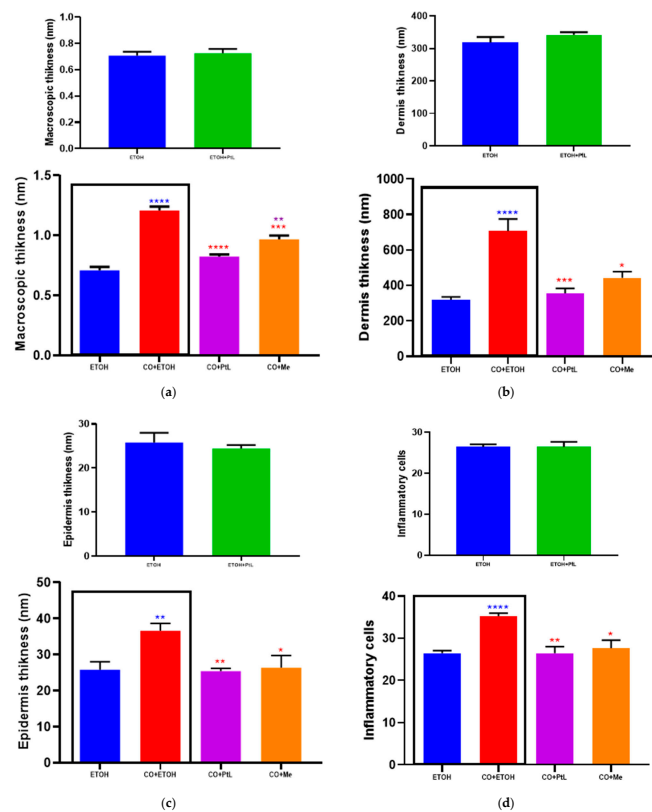


Figure 3. Changes in macroscopic ear (a), dermis (b) and epidermis thickness (c) and the number of inflammatory cells in the rats' ears (d) after the croton oil challenge test. Differences between the ETOH and ETOH + PtL and the ETOH and CO + ETOH groups were assessed using a Student's T-test, while differences between CO + ETOH, CO + PtL, and CO + Me were assessed using an one-way ANOVA. (ETOH: control animals, application of pure ethanol; CO + ETOH: croton oil 5% dissolved in pure ethanol; ETOH + PtL; application of *P. tridentatum* extract dissolved in pure ethanol; CO + Me: croton oil 5% dissolved in pure ethanol followed by application of Medrol 15 min later; CO + PtL: croton oil 5% dissolved in pure ethanol followed by application of *P. tridentatum* extract 15 min later). Results are expressed as mean \pm SEM. Symbols are colored according to their respective experimental group. Results are expressed as mean \pm SEM. * $p < 0.05$, ** $p < 0.01$, *** $p < 0.001$, **** $p < 0.0001$.

3.3. Histopathological Assessment of Ear Samples

The application of *P. tridentatum* extract alone (ETOH + PtL) did not significantly alter dermis (Figure 3b: $t(8) = 1.285$, $p = 0.2347$) and epidermis (Figure 3c: $t(8) = 0.5749$, $p = 0.5812$) thickness when compared to the control group (ETOH). Croton oil application (CO + ETOH) significantly increased dermis (Figure 3b: $t(8) = 5.481$, $p = 0.0006$) and epidermis (Figure 3c: $t(8) = 3.560$, $p = 0.0003$) thickness in comparison with the ETOH group.

Similarly to what was observed previously, ear thickness was significantly decreased after topical application of *P. tridentatum* extract (CO + PtL, ANOVA one-way: $F(2,13) = 16.05$, $p = 0.0003$) and Medrol (CO + Me, ANOVA one-way: $F(2,13) = 7.686$, $p = 0.0063$).

Additionally, the application of *P. tridentatum* extract alone (ETOH + PtL) did not significantly alter the number of inflammatory cells in the ear samples (Figure 3d: $t(8) = 0.00$, $p > 0.9999$) when compared to the control group, while the application of croton oil significantly increased it (Figure 3d: $t(8) = 8.976$, $p < 0.0001$). Finally, further analysis showed significant differences after treatment (Figure 3d: ANOVA one-way: $F(2,13) = 9.728$, $p = 0.0026$), with post hoc tests showing that the application of *P. tridentatum* extract and Medrol significantly decreased the number of inflammatory cells.

3.4. Mechanical Hyperalgesia

To evaluate the development of mechanical hyperalgesia, the PAM test was performed. Statistical analysis of PAM showed mechanical hyperalgesia in the ipsilateral knee varied differently throughout the experimental period depending of the experimental group (Figure 4; ANOVA two-way: Interaction: $F(16,90) = 6.941$, $p < 0.0001$; Time: $F(4,90) = 23.11$, $p < 0.0001$; Group: $F(4,90) = 36.634$, $p < 0.0001$). Post hoc tests showed OA animals displayed greater levels of mechanical hyperalgesia when compared to shams during weeks one to four. Post hoc tests also showed both extract treatments significantly decreased mechanical hyperalgesia during weeks three to four when compared to non-treated OA animals. Additionally, the treatment with the commercial non-steroidal anti-inflammatory drug partially reverts mechanical hyperalgesia when compared to non-treated OA animals.

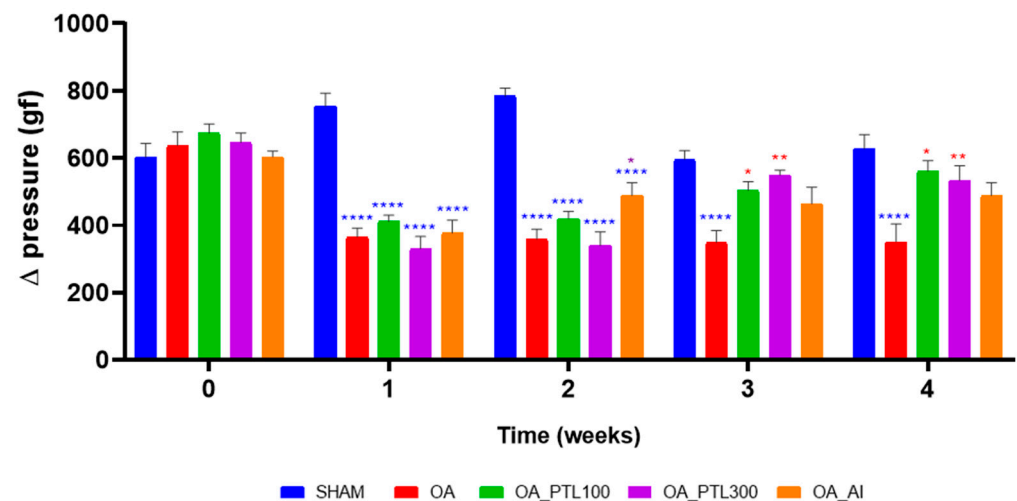


Figure 4. Assessment of mechanical hyperalgesia in the knee throughout the experimental period. Symbols are colored according to their respective experimental group. Differences between the sham, OA, OA_PtL100, OA_PtL300, and OA_AI groups were assessed using a two-way ANOVA. Results are expressed as mean \pm SEM. * $p < 0.05$, ** $p < 0.01$, **** $p < 0.0001$ ($n_{\text{SHAM}} = 4$; $n_{\text{OA}} = 4$; $n_{\text{OA_PTL100}} = 5$; $n_{\text{OA_PTL300}} = 5$; $n_{\text{OA_AI}} = 5$) (SHAM—control animals that underwent all surgical procedures but were not induced OA; OA—osteoarthritic animals; OA_PTL100—osteoarthritic animal that from week two were treated with a concentration of 100 mg/kg of *Pterospartum tridentatum* extract; OA_PTL300—osteoarthritic animals that, from week two, were treated with a concentration of 300 mg/kg of *Pterospartum tridentatum* extract; OA_AI—osteoarthritic animal that, from week two, were treated with a commercial nonsteroidal anti-inflammatory drug).

3.5. Perimeter of Knee

To evaluate inflammation of the knee, the knee's perimeter was assessed (Figure 5). Statistical analysis showed the edema in the ipsilateral knee varied differently throughout the experimental period depending on the experimental group (ANOVA_{two-way}: Interaction: $F(8,54) = 1.694$, $p = 0.01210$; Time: $F(2,54) = 51.98$, $p < 0.0001$; Group: $F(4,54) = 4.383$, $p = 0.0038$). Post hoc tests showed OA animals displayed increased knee perimeter when compared to shams during weeks one to four. Moreover, both extract treatments partially reverted the knee swelling when compared to non-treated OA animals. Treatment with the commercial non-steroidal anti-inflammatory drug also partially reverted knee oedema when compared to non-treated OA animals, but only in the fourth week.

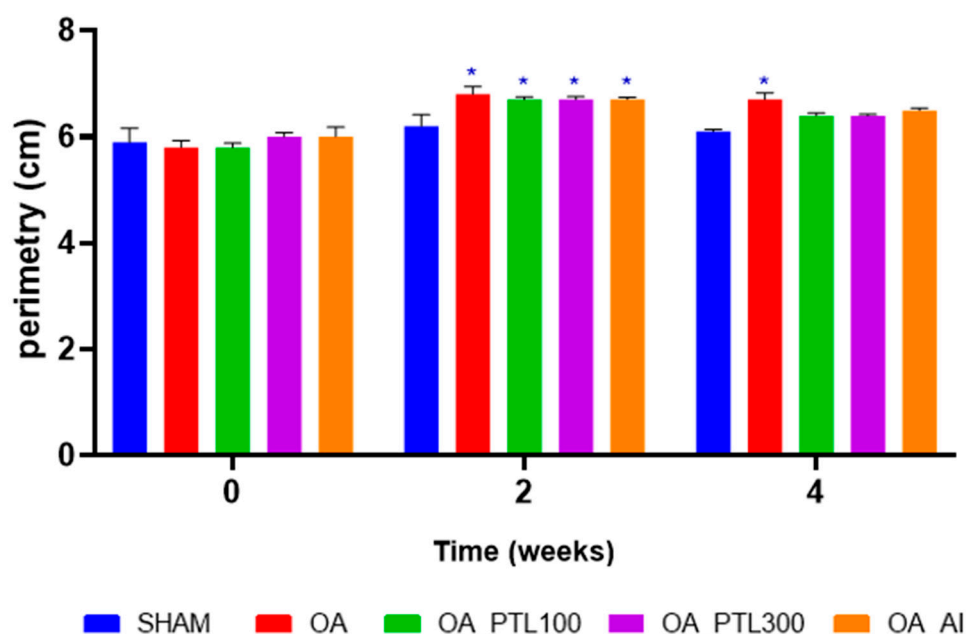


Figure 5. Assessment of knee perimeter throughout the experimental period. Symbols are colored according to their respective experimental group. Differences between the sham, OA, OA_PtL100, OA_PtL300, and OA_AI groups were assessed using a two-way ANOVA. Results are expressed as mean \pm SEM. * $p < 0.05$ $n_{\text{SHAM}} = 4$; $n_{\text{OA}} = 4$; $n_{\text{OA_PTL100}} = 5$; $n_{\text{OA_PTL300}} = 5$; $n_{\text{OA_AI}} = 5$ (SHAM—control animals that underwent all surgical procedures but were not induced OA; OA—osteoarthritic animals; OA_PTL100—osteoarthritic animals that from week two were treated with a concentration of 100 mg/kg of *Pterospartum tridentatum* extract; OA_PTL300—osteoarthritic animals that from week two were treated with a concentration of 300 mg/kg of *Pterospartum tridentatum* extract; OA_AI—osteoarthritic animals that from week two were treated with a commercial nonsteroidal anti-inflammatory drug).

3.6. Molecular Docking Analysis

The molecular docking studies of quercetin, isoquercetin, and genistein were performed against the crystal structure of PPAR α (PDB 2P54) and PPAR γ (PDB 6TSG), respectively), mPGES-1 (PDB 4YL1), prostaglandin H (2) Synthase-1 (PDB 1Q4G), protein kinase CK2 α (PDB 6TGU), inhibitor-bound human 5-lipoxygenase-activating protein (PDB 2Q7M), and the crystal structure of mPGES-1 bound to inhibitor (PDB 5T36) to determine their binding affinities. The results are synthesized in Table 2 and Figure 6.

Table 2. Molecular docking results of isoquercetin, genistein, and quercetin against crystal structure of peroxisome proliferator-activated receptor alpha and gamma (PPAR α (PDB 2P54) and PPAR γ (PDB 6TSG), respectively), mPGES-1 (PDB 4YL1), prostaglandin H (2) Synthase-1 (PDB 1Q4G), protein kinase CK2 α (PDB 6TGU), inhibitor-bound human 5-lipoxygenase-activating protein (PDB 2Q7M), and the crystal structure of mPGES-1 bound to inhibitor (PDB 5T36).

Protein	Compound	Binding Energy (kcal/mol)	Inhibition Konstant (μ M)	Intermolecular Energy (kcal/mol)
PPAR γ (PDB 6tsg)	Isoquercetin	−7.24	4.91	−10.82
	Quercetin	−6.23	26.93	−10.11
	Genistein	−5.81	55.18	−9.09
COX-2 (PDB 4y11)	Isoquercetin	−4.66	385.08	−8.24
	Quercetin	−4.79	310.18	−8.66
	Genistein	−4	1160	−7.28
COX-1 (PDB 1q4g)	Isoquercetin	−5.98	41.07	−9.56
	Quercetin	−9.01	0.24772	−10.80
	Genistein	−8.78	0.36957	−9.97
PPAR α (PDB 2p54)	Isoquercetin	−7.27	4.68	−10.85
	Quercetin	−5.66	71.17	−9.54
	Genistein	−6.24	26.76	−9.52
CK2 α (PDB 6tgu)	Isoquercetin	−8.66	0.44756	−12.08
	Quercetin	−9.97	0.04941	−11.76
	Genistein	−9.78	0.06758	−10.98
5-LO (PDB 2q7m)	Isoquercetin	−7.96	1.46	−11.54
	Quercetin	−6.92	8.43	−10.80
	Genistein	−6.87	9.19	−10.15
mPGES-1 (PDB 5t36)	Isoquercetin	−4.62	410.41	−8.2
	Quercetin	−1.52	5457	−5.6
	Genistein	−5.04	201.89	−8.32

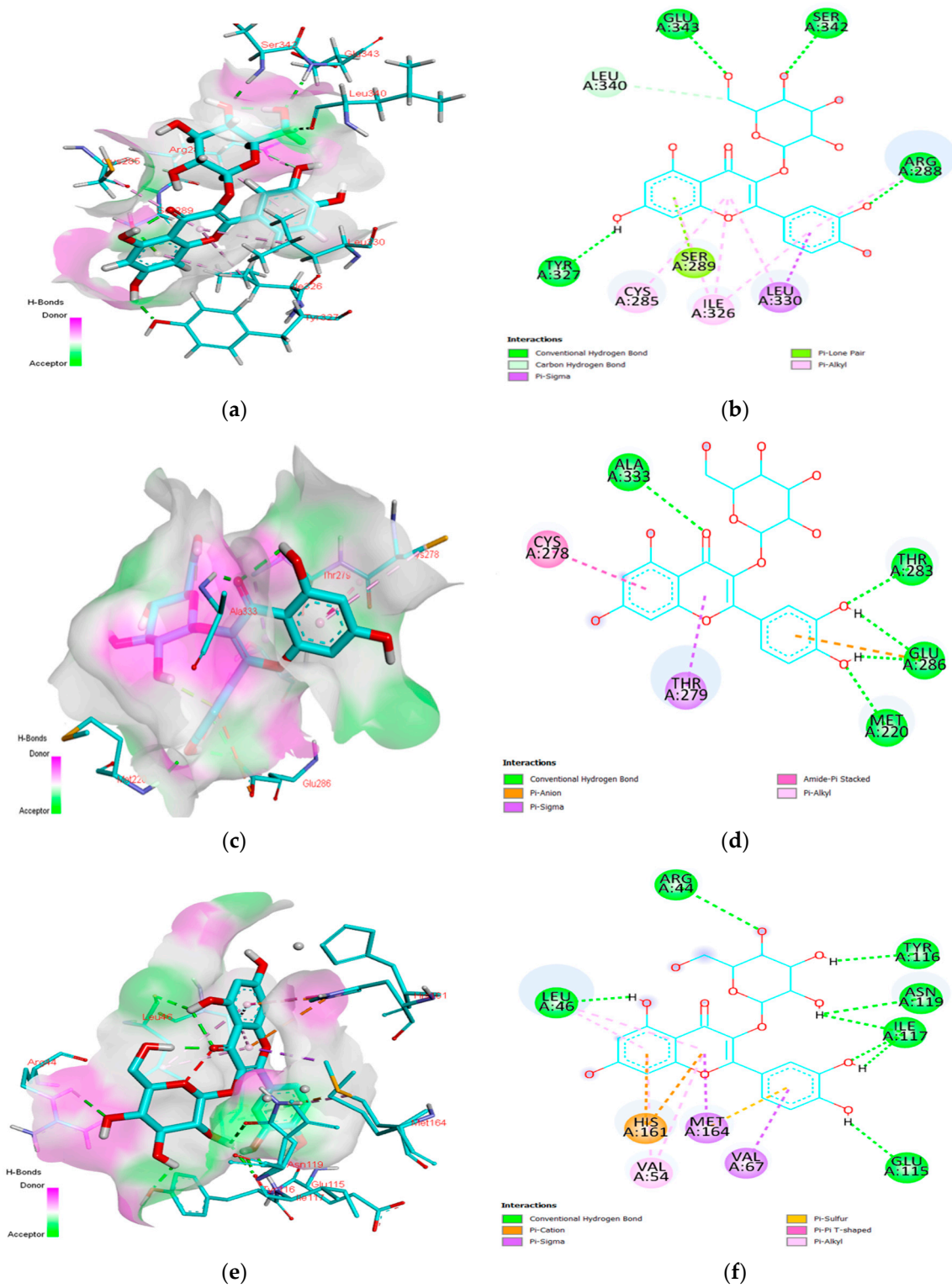


Figure 6. Cont.

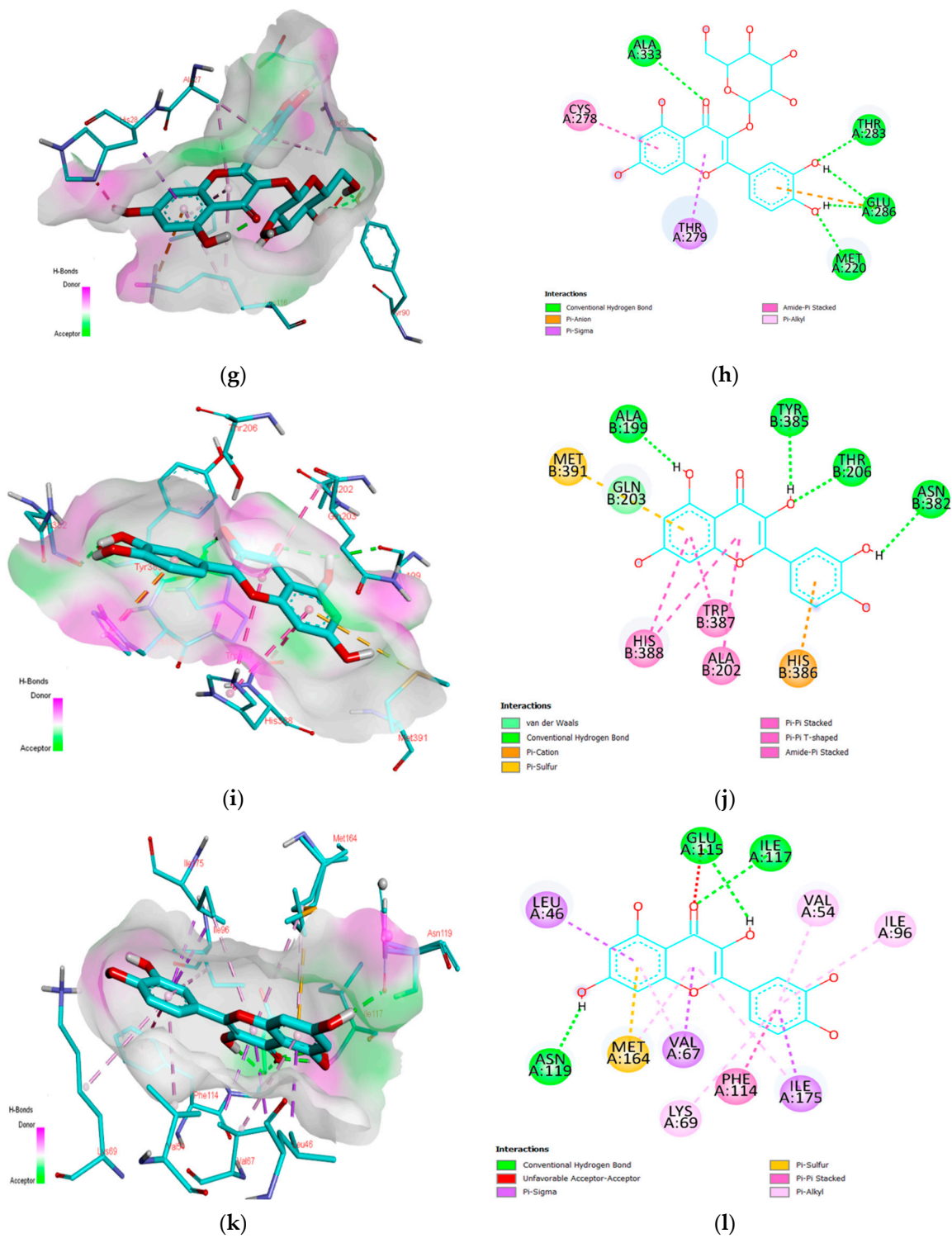


Figure 6. Cont.

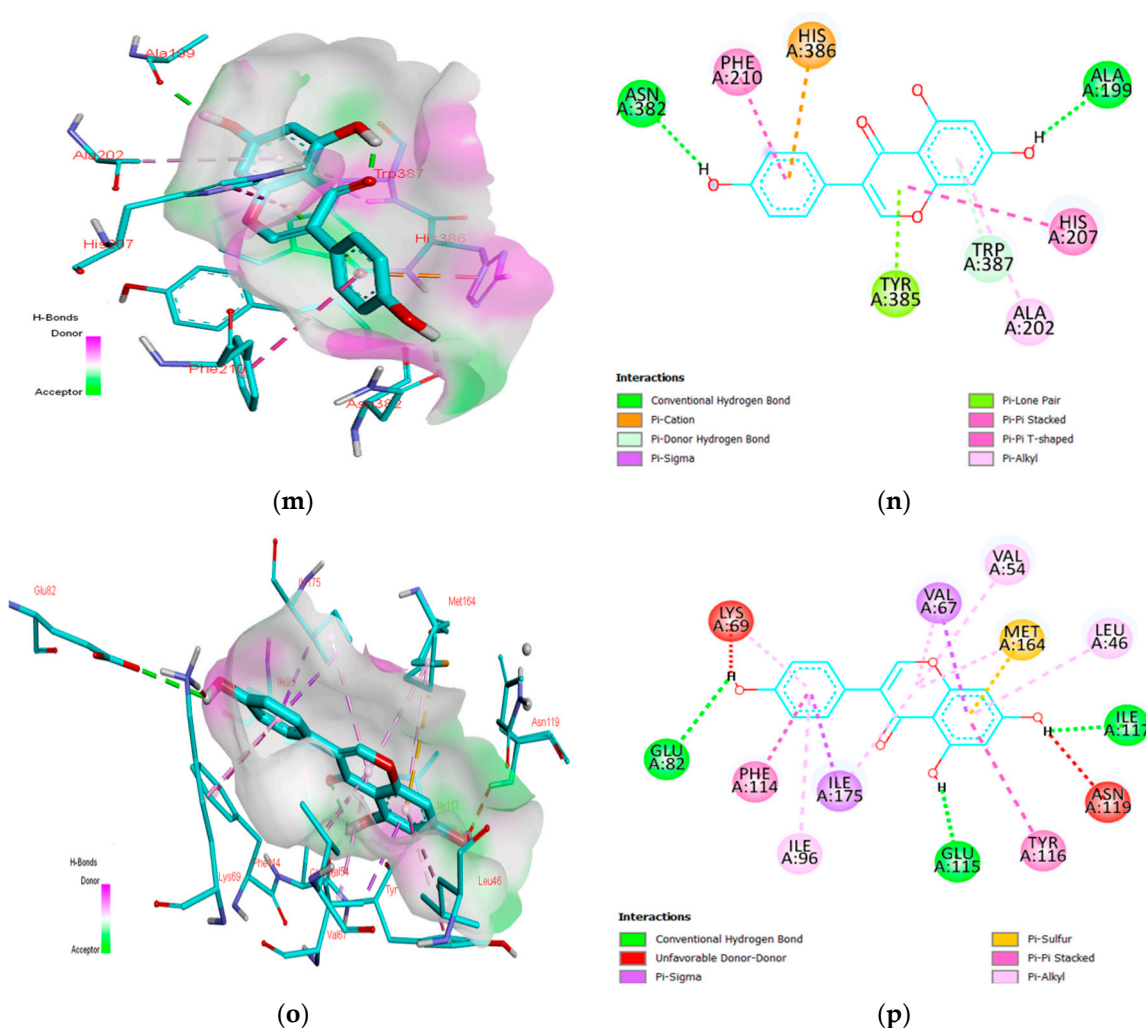


Figure 6. Schematic representation of the interaction of isoquercetin ligand on the active site of PPAR γ (PDB 6tsg) receptor in 3D (a) and 2D (b) structure; PPAR α (PDB 2P54) receptor in three-dimensional (c) and two-dimensional (d) structure; CK2 α (PDB 6TGU) receptor in three-dimensional (e) and two-dimensional (f) structure; 5-lipoxygenase-activating protein (PDB 2Q7M) receptor in 3D (g) and 2D (h) structure; interaction of quercetin and genistein ligand on the active site of prostaglandin H (2) synthase-1 (PDB 1Q4G) in three-dimensional (i,m, respectively) and two-dimensional (j,n, respectively) structure and CK2 α (PDB 6TGU) receptor in three-dimensional (k,o, respectively) and two-dimensional (l,p, respectively) structure.

Isoquercetin demonstrated strong molecular interactions with PPAR γ , PPAR α , CK2 α , and 5-LO proteins (binding energies of -7.24 , -7.27 , -8.66 , and -7.96 kcal/mol, respectively). Genistein and quercetin had docking for Ck2a (binding energies of -9.97 and -9.78 , respectively) and COX-1 (binding energies of -9.01 and -8.78 , respectively).

4. Discussion

P. tridentatum is known as displaying anti-inflammatory activity, with fresh or shade-dried flowers of *P. tridentatum* also being used in traditional medicine, in infusions, decoctions, and tonics [26] as anti-inflammatory [11,12], diuretic, and depurative of the liver [8,14,27,28].

Herein, we evaluated the effects of the leaves methanolic extract of *P. tridentatum* using various in vivo tests in rodents, as well as computational models to assess the molecular interaction of its biological compounds with proteins involved in inflammatory cascades.

Our data shows the topical application (100 mg/mL) and oral administration (100 and 300 mg/kg) of *P. tridentatum* extract were able to significantly decrease ear and knee oedema, respectively, as well as mechanical hyperalgesia. Moreover, the molecular docking analysis evaluated the binding of the compounds (isoquercetin, quercetin, and genistein) with amino acid residues at the mentioned proteins active site and measured binding free energy parameter, inhibition constants, hydrogen bonding, and interactions. The free energy value can predict a compound's binding affinity and its ability to inhibit the protein. A negative free energy value indicates a stronger affinity between the ligands and receptors [24]. Based on the results in Table 2, isoquercetin, quercetin, and genistein had lower inhibition constant, negative free binding, and negative intermolecular interaction energies, indicating stronger affinity with the receptors and that they could potentially inhibit the activation of inflammatory cascade.

Regarding the in vivo experiment of acute inflammation, the ear oedema induced by topical administration of croton oil mimics several characteristics observed in human skin diseases [16]. In the used model, the application of croton oil provokes an inflammatory reaction, specifically epidermal hyperplasia, increased vascularization, and increased inflammatory infiltrates [29]. After croton oil application, the ears' histopathological analysis revealed an increase in ear thickness (macroscopic and microscopic), as well, regarding the number of inflammatory cells. This effect was prevented by the topical application of *P. tridentatum* extract, which did not affect ear macro- and microstructure when applied alone. Moreover, its effects were the same as Medrol application, a synthetic glucocorticoid used to treat local inflammation [30].

In the chronic inflammation model, the K/C-induced experimental osteoarthritis causes inflammation in the knee joint and subsequent chronic pain [20,30]. The PAM data showed the animals developed mechanical hyperalgesia in the knee, confirming the correct induction of the model. This effect was sustained from the first week after induction and lasted until the end of the experiment. Importantly, our results showed both concentrations of the extract (100 and 300 mg/Kg) were able to decrease mechanical allodynia from the third week onwards (one week after the start of treatment). Moreover, the extract was more efficient than the commercial non-steroidal anti-inflammatory drug used as a control for drug administration (ibuprofen). As with the PAM, the knee perimeter is an essential measure to confirm experimental OA, as this test, by measuring the knee perimeter, measures oedema and indirectly inflammation [22,31]. Previous studies showed that K/C-induced osteoarthritis causes inflammation and swelling in the knee [20,32]. Our outcomes are in line with previous results, since, after OA induction, the knee perimeter of rats increased [20]. Similarly, to what was observed in the PAM test, both the extract treatments and the nonsteroidal anti-inflammatory drug treatment decreased knee perimeter in OA animals. Furthermore, both extract concentrations displayed identical efficiency.

The phytochemical characterization of *P. tridentatum* demonstrated its richness in phenolic compounds, which are frequently associated with anti-inflammatory activity [11,33,34]. In the present study, the HPLC-DAD analysis of *P. tridentatum* leaves methanolic extract demonstrated the presence of various phytochemical compounds, predominantly quercetin, quercetin derivatives, isoquercetin, and genistein. These outcomes agree with the phytochemical studies found in the literature, which describe the occurrence of these types of compounds in extracts of *P. tridentatum* [25,35,36].

Phenolic compounds can act alone or by synergy to protect against damage caused by oxidative stress. In their structure, phenolic compounds display an aromatic ring that presents one or more hydroxyl substitutes, including their functional derivatives. This aromatic feature in association with a highly conjugated system with multiple hydroxyl groups makes these compounds good electron or hydrogen atom donors and enhances their ability to neutralize free radicals and other reactive oxygen species [37].

As previously shown, isoquercetin and genistein, phenolic compounds present in *P. tridentatum* extracts, could be linked to the scavenging of reactive oxygen species [38–40]. Nevertheless, our results in molecular docking analysis showed isoquercetin can also act as

an agonist of PPAR α and PPAR γ , inhibiting NF- κ B signaling and activation of macrophages, consequently decreasing inflammatory cytokine production (tumor necrosis factor-alpha (TNF- α), interleukin (IL)-6, and IL-1 β [41]. Furthermore, isoquercetin showed an important capability to inhibit 5-LO, which decreases TNF- α , IL-6, and MCP-1 production, and it is also involved in inflammation [42]. Additionally, isoquercetin and genistein demonstrated very strong molecular interactions with CK2 α , which is known to inhibit NF- κ B activation in macrophages and subsequently IL-1, IL-6, and IL-10 cytokine secretion [43,44]. Finally, the inhibition of COX-1 by quercetin and genistein can act by decreasing the levels of arachidonic acid, thus decreasing the production of bioactive prostanoids [45,46].

In the literature, studies about the effect of *P. tridentatum* on inflammation are scarce and do not identify the mechanism of action, but some reports support our results. Bremner et al. [11] evaluated the anti-inflammatory activity of *P. tridentatum* (methanolic, petroleum ether, and ethyl acetate extracts), and their results demonstrated the inhibition of TNF- α levels in human monocytes. Likewise, Simões et al. [47] assessed the anti-inflammatory activity of *P. tridentatum* ethanolic extracts and demonstrated a downregulation of the Nos2 gene, along with a decrease in the transcription of the pro-inflammatory genes IL1b, IL6, and Ptgs2.

5. Conclusions

Our work highlights the potential of *P. tridentatum* extracts as a source of compounds that can be used as adjuvants in the management of pain and inflammation. However, further studies should evaluate the long-term effect of the extracts to check their contribution to preventing OA progression and its efficiency in other experimental models of inflammation. In addition, it would also be interesting to test a larger range of extract concentrations to determine the lowest concentration that maintains anti-inflammatory effects.

Author Contributions: I.M.L.: Conceptualization, Data curation, Formal analysis, Investigation, Methodology, Writing—original draft. J.N.D.G. and N.M.: Investigation, Data curation. C.G. and M.S.: Investigation. A.C.P.D.: Project administration, Supervision, Methodology. F.P.-R.: Funding acquisition, Project administration, Supervision, Methodology, Writing—review and editing. All authors have read and agreed to the published version of the manuscript.

Funding: This work was funded by ICVS Scientific Microscopy Platform, a member of the national infrastructure PPBI—Portuguese Platform of Bioimaging (PPBI-POCI-01-0145-FEDER-022122), by National funds, through the Foundation for Science and Technology (FCT)—project UIDB/50026/2020 and UIDP/50026/2020, and by the projects NORTE-01-0145-FEDER-000039 and NORTE-01-0145-FEDER-085468, supported by Norte Portugal Regional Operational Programme (NORTE 2020) under the PORTUGAL 2020 Partnership Agreement, through the European Regional Development Fund (ERDF). IL was supported by grants from FCT PhD programs (PD/BD/150263/2019).

Institutional Review Board Statement: The experimental protocol was approved by the Institutional and National Ethical Commission (DGAV 23875/2019) and followed the European Community Council Directive 2010/63/EU concerning the use of animals for scientific purposes.

Informed Consent Statement: Not applicable.

Data Availability Statement: The data presented in this study are available upon request from the corresponding author.

Conflicts of Interest: The authors declare no conflict of interest.

References

1. Freire, M.O.; Van Dyke, T.E. Natural resolution of inflammation. *Periodontology 2000* **2013**, *63*, 149–164. [[CrossRef](#)] [[PubMed](#)]
2. Furman, D.; Campisi, J.; Verdin, E.; Carrera-Bastos, P.; Targ, S.; Franceschi, C.; Ferrucci, L.; Gilroy, D.W.; Fasano, A.; Miller, G.W.; et al. Chronic inflammation in the etiology of disease across the life span. *Nat. Med.* **2019**, *25*, 1822–1832. [[CrossRef](#)] [[PubMed](#)]
3. Tabas, I.; Glass, C.K. Anti-Inflammatory Therapy in Chronic Disease: Challenges and Opportunities. *Science* **2013**, *339*, 166–172. [[CrossRef](#)]
4. Tolba, R. Nonsteroidal Anti-inflammatory Drugs (NSAIDs). In *Treatment of Chronic Pain Conditions: A Comprehensive Handbook*; Pope, J., Deer, T., Eds.; Springer: New York, NY, USA, 2017; pp. 77–79. [[CrossRef](#)]

5. Rahman, M.; Rahaman, S.; Islam, R.; Rahman, F.; Mithi, F.M.; Alqahtani, T.; Almikhlaifi, M.A.; Alghamdi, S.Q.; Alruwaili, A.S.; Hossain, S.; et al. Role of Phenolic Compounds in Human Disease: Current Knowledge and Future Prospects. *Molecules* **2022**, *27*, 233. [[CrossRef](#)]
6. Khanna, D.; Sethi, G.; Ahn, K.S.; Pandey, M.K.; Kunnumakkara, A.B.; Sung, B.; Aggarwal, A.; Aggarwal, B.B. Natural products as a gold mine for arthritis treatment. *Curr. Opin. Pharmacol.* **2007**, *7*, 344–351. [[CrossRef](#)]
7. Tungmunnithum, D.; Thongboonyou, A.; Pholboon, A.; Yangsabai, A. Flavonoids and Other Phenolic Compounds from Medicinal Plants for Pharmaceutical and Medical Aspects: An Overview. *Medicines* **2018**, *5*, 93. [[CrossRef](#)]
8. Coelho, M.T.; Gonçalves, J.C.; Alves, V.; Moldão-Martins, M. Antioxidant activity and phenolic content of extracts from different *Pterospartum tridentatum* populations growing in Portugal. *Procedia Food Sci.* **2011**, *1*, 1454–1458. [[CrossRef](#)]
9. Ferreira, F.M.; Dinis, L.T.; Azedo, P.; Galhano, C.I.; Simões, A.; Cardoso, S.M.; Rosário, M.; Domingues, M.; Pereira, O.R.; Palmeira, C.M.; et al. Antioxidant capacity and toxicological evaluation of *Pterospartum tridentatum* flower extracts. *CyTA—J. Food* **2012**, *10*, 92–102. [[CrossRef](#)]
10. Ribeiro, J.A.; Monteiro, A.M.; da Fonseca Silva, M.D. *Etnobotânica: Plantas Bravias Comestíveis, Condimentares e Mediciniais*, 2nd ed.; J. Azevedo: Mirandela, Portugal, 2000; p. 96. ISBN 9729001448.
11. Bremner, P.; Rivera, D.; Calzado, M.; Obón, C.; Inocencio, C.; Beckwith, C.; Fiebich, B.; Muñoz, E.; Heinrich, M. Assessing medicinal plants from South-Eastern Spain for potential anti-inflammatory effects targeting nuclear factor-Kappa B and other pro-inflammatory mediators. *J. Ethnopharmacol.* **2009**, *124*, 295–305. [[CrossRef](#)] [[PubMed](#)]
12. Gião, M.S.; González-SanJosé, M.L.; Rivero-Pérez, M.D.; Pereira, C.I.; Pintado, M.M.; Malcata, F.X. Infusions of Portuguese medicinal plants: Dependence of final antioxidant capacity and phenol content on extraction features. *J. Sci. Food Agric.* **2007**, *87*, 2638–2647. [[CrossRef](#)]
13. Luís, Â.; Domingues, F.; Duarte, A.P. Bioactive Compounds, RP-HPLC Analysis of Phenolics, and Antioxidant Activity of Some Portuguese Shrub Species Extracts. *Nat. Prod. Commun.* **2011**, *6*, 1863–1872. [[CrossRef](#)]
14. Aires, A.; Marrinhas, E.; Carvalho, R.; Dias, C.; Saavedra, M.J. Phytochemical Composition and Antibacterial Activity of Hydroalcoholic Extracts of *Pterospartum tridentatum* and *Mentha pulegium* against *Staphylococcus aureus* Isolates. *BioMed Res. Int.* **2016**, *2016*. [[CrossRef](#)]
15. Dias, A.C.P.; Seabra, R.M.; Andrade, P.B.; Fernandes-Ferreira, M. The development and evaluation of an hplc-dad method for the analysis of the phenolic fractions from in vivo and in vitro biomass of *hypericum* species. *J. Liq. Chromatogr. Relat. Technol.* **2007**, *22*, 215–227. [[CrossRef](#)]
16. Rodrigues, K.C.; Chibli, L.A.; Santos, B.C.; Temponi, V.S.; Pinto, N.C.; Scio, E.; Del-Vechio-Vieira, G.; Alves, M.S.; Sousa, O.V. Evidence of Bioactive Compounds from Vernonia polyanthes Leaves with Topical Anti-Inflammatory Potential. *Int. J. Mol. Sci.* **2016**, *17*, 1929. [[CrossRef](#)] [[PubMed](#)]
17. Oliveira, J.M.; Kotobuki, N.; Tadokoro, M.; Hirose, M.; Mano, J.F.; Reis, R.L.; Ohgushi, H. Ex vivo culturing of stromal cells with dexamethasone-loaded carboxymethylchitosan/poly(amidoamine) dendrimer nanoparticles promotes ectopic bone formation. *Bone* **2010**, *46*, 1424–1435. [[CrossRef](#)] [[PubMed](#)]
18. Pinto-Ribeiro, F.; Amorim, D.; David-Pereira, A.; Monteiro, A.M.; Costa, P.; Pertovaara, A.; Almeida, A. Pronociception from the dorsomedial nucleus of the hypothalamus is mediated by the rostral ventromedial medulla in healthy controls but is absent in arthritic animals. *Brain Res. Bull.* **2013**, *99*, 100–108. [[CrossRef](#)]
19. David-Pereira, A.; Puga, S.; Gonçalves, S.; Amorim, D.; Silva, C.; Pertovaara, A.; Almeida, A.; Pinto-Ribeiro, F. Metabotropic glutamate 5 receptor in the infralimbic cortex contributes to descending pain facilitation in healthy and arthritic animals. *Neuroscience* **2016**, *312*, 108–119. [[CrossRef](#)]
20. Amorim, D.; David-Pereira, A.; Pertovaara, A.; Almeida, A.; Pinto-Ribeiro, F. Amitriptyline reverses hyperalgesia and improves associated mood-like disorders in a model of experimental monoarthritis. *Behav. Brain Res.* **2014**, *265*, 12–21. [[CrossRef](#)]
21. Malfait, A.M.; Little, C.B.; McDougall, J.J. A commentary on modelling osteoarthritis pain in small animals. *Osteoarthr. Cartil.* **2013**, *21*, 1316–1326. [[CrossRef](#)]
22. Barton, N.J.; Strickland, I.T.; Bond, S.M.; Brash, H.M.; Bate, S.T.; Wilson, A.W.; Chessell, I.P.; Reeve, A.J.; McQueen, D.S. Pressure application measurement (PAM): A novel behavioural technique for measuring hypersensitivity in a rat model of joint pain. *J. Neurosci. Methods* **2007**, *163*, 67–75. [[CrossRef](#)] [[PubMed](#)]
23. Adães, S.; Ferreira-Gomes, J.; Mendonça, M.; Almeida, L.; Castro-Lopes, J.M.; Neto, F.L. Injury of primary afferent neurons may contribute to osteoarthritis induced pain: An experimental study using the collagenase model in rats. *Osteoarthr. Cartil.* **2015**, *23*, 914–924. [[CrossRef](#)]
24. Hendriani, R.; Nursamsiar, N.; Tjitraesmi, A. In Vitro and in silico evaluation of xanthine oxidase inhibitory activity of quercetin contained in sonchus arvensis leaf extract. *Asian J. Pharm. Clin. Res.* **2017**, *50*–53. [[CrossRef](#)]
25. Roriz, C.L.; Barros, L.; Carvalho, A.M.; Santos-Buelga, C.; Ferreira, I.C. Scientific validation of synergistic antioxidant effects in commercialised mixtures of *Cymbopogon citratus* and *Pterospartum tridentatum* or *Gomphrena globosa* for infusions preparation. *Food Chem.* **2015**, *185*, 16–24. [[CrossRef](#)] [[PubMed](#)]
26. Pinela, J.; Barros, L.; Carvalho, A.M.; Ferreira, I.C. Influence of the drying method in the antioxidant potential and chemical composition of four shrubby flowering plants from the tribe Genisteae (Fabaceae). *Food Chem. Toxicol.* **2011**, *49*, 2983–2989. [[CrossRef](#)] [[PubMed](#)]

27. Grosso, A.C.; Costa, M.M.; Ganço, L.; Pereira, A.L.; Teixeira, G.; Lavado, J.M.; Figueiredo, A.C.; Barroso, J.G.; Pedro, L.G. Essential oil composition of *Pterospartum tridentatum* grown in Portugal. *Food Chem.* **2007**, *102*, 1083–1088. [[CrossRef](#)]
28. Gonçalves, S.; Gomes, D.; Costa, P.; Romano, A. The phenolic content and antioxidant activity of infusions from Mediterranean medicinal plants. *Ind. Crops Prod.* **2013**, *43*, 465–471. [[CrossRef](#)]
29. Di Meglio, P.; Perera, G.K.; Nestle, F.O. The Multitasking Organ: Recent Insights into Skin Immune Function. *Immunity* **2011**, *35*, 857–869. [[CrossRef](#)]
30. Barnes, P.J. How corticosteroids control inflammation: Quintiles Prize Lecture 2005. *Br. J. Pharmacol.* **2006**, *148*, 245–254. [[CrossRef](#)] [[PubMed](#)]
31. Neugebauer, V.; Han, J.S.; Adwanikar, H.; Fu, Y.; Ji, G. Techniques for Assessing Knee Joint Pain in Arthritis. *Mol. Pain* **2007**, *3*, 8. [[CrossRef](#)] [[PubMed](#)]
32. Mussawy, H.; Zustin, J.; Luebke, A.M.; Strahl, A.; Krenn, V.; Rütther, W.; Rolvien, T. The histopathological synovitis score is influenced by biopsy location in patients with knee osteoarthritis. *Arch. Orthop. Trauma Surg.* **2021**, *142*, 2991–2997. [[CrossRef](#)]
33. Pinto, D.C.; Simões, M.A.; Silva, A.M. *Genista tridentata* L.: A Rich Source of Flavonoids with Anti-Inflammatory Activity. *Medicines* **2020**, *7*, 31. [[CrossRef](#)] [[PubMed](#)]
34. Ferrandiz, M.L.; Alcaraz, M. Anti-inflammatory activity and inhibition of arachidonic acid metabolism by flavonoids. *Agents Actions* **1991**, *32*, 283–288. [[CrossRef](#)]
35. Roriz, C.L.; Barros, L.; Carvalho, A.M.; Santos-Buelga, C.; Ferreira, I.C. *Pterospartum tridentatum*, *Gomphrena globosa* and *Cymbopogon citratus*: A phytochemical study focused on antioxidant compounds. *Food Res. Int.* **2014**, *62*, 684–693. [[CrossRef](#)]
36. Caleja, C.; Finimundy, T.C.; Pereira, C.; Barros, L.; Calhelha, R.C.; Sokovic, M.; Ivanov, M.; Carvalho, A.M.; Rosa, E.; Ferreira, I.C. Challenges of traditional herbal teas: Plant infusions and their mixtures with bioactive properties. *Food Funct.* **2019**, *10*, 5939–5951. [[CrossRef](#)]
37. Zhang, H.; Tsao, R. Dietary polyphenols, oxidative stress and antioxidant and anti-inflammatory effects. *Curr. Opin. Food Sci.* **2016**, *1*, 33–42. [[CrossRef](#)]
38. Goh, Y.X.; Jalil, J.; Lam, K.W.; Husain, K.; Premakumar, C.M. Genistein: A Review on its Anti-Inflammatory Properties. *Front. Pharmacol.* **2022**, *13*. [[CrossRef](#)]
39. Elnoury, H.A. Isoquercetin Could Protect Against Ovariectomy-Induced Neuronal Changes in Rats. *Egypt. J. Basic Clin. Pharmacol.* **2019**, *9*. [[CrossRef](#)]
40. Yang, Q.; Kang, Z.; Zhang, J.; Qu, F.; Song, B. Neuroprotective effects of isoquercetin: An in vitro and in vivo study. *Cell J.* **2021**, *23*, 355. [[CrossRef](#)]
41. Decara, J.; Rivera, P.; López-Gambero, A.J.; Serrano, A.; Pavón, F.J.; Baixeras, E.; De Fonseca, F.R.; Suárez, J. Peroxisome Proliferator-Activated Receptors: Experimental Targeting for the Treatment of Inflammatory Bowel Diseases. *Front. Pharmacol.* **2020**, *11*, 730. [[CrossRef](#)]
42. Mohd Amin, S.N.; Idris, M.H.; Selvaraj, M.; Mohd Amin, S.N.; Jamari, H.; Kek, T.L.; Salleh, M.Z. Virtual screening, ADME study, and molecular dynamic simulation of chalcone and flavone derivatives as 5-Lipoxygenase (5-LO) inhibitor. *Mol. Simul.* **2020**, *46*, 487–496. [[CrossRef](#)]
43. Glushkova, O.V.; Parfenyuk, S.B.; Novoselova, T.V.; Khrenov, M.O.; Lunin, S.M.; Novoselova, E.G. The Role of p38 and CK2 Protein Kinases in the Response of RAW 264.7 Macrophages to Lipopolysaccharide. *Biochemistry* **2018**, *83*, 746–754. [[CrossRef](#)] [[PubMed](#)]
44. Larson, S.R.; Bortell, N.; Illies, A.; Crisler, W.J.; Matsuda, J.L.; Lenz, L.L. Myeloid Cell CK2 Regulates Inflammation and Resistance to Bacterial Infection. *Front. Immunol.* **2020**, *11*. [[CrossRef](#)] [[PubMed](#)]
45. Calvello, R.; Lofrumento, D.D.; Perrone, M.G.; Cianciulli, A.; Salvatore, R.; Vitale, P.; De Nuccio, F.; Giannotti, L.; Nicolardi, G.; Panaro, M.A.; et al. Highly Selective Cyclooxygenase-1 Inhibitors P6 and Mofezolac Counteract Inflammatory State both In Vitro and In Vivo Models of Neuroinflammation. *Front. Neurol.* **2017**, *8*, 251. [[CrossRef](#)] [[PubMed](#)]
46. Schmid, T.; Brüne, B. Prostanoids and resolution of inflammation—beyond the lipid-mediator class switch. *Front. Immunol.* **2021**, *12*. [[CrossRef](#)]
47. Simões, M.A.; Pinto, D.C.; Neves, B.M.; Silva, A.M. Flavonoid Profile of the *Genista tridentata* L., a Species Used Traditionally to Treat Inflammatory Processes. *Molecules* **2020**, *25*, 812. [[CrossRef](#)]

Disclaimer/Publisher’s Note: The statements, opinions and data contained in all publications are solely those of the individual author(s) and contributor(s) and not of MDPI and/or the editor(s). MDPI and/or the editor(s) disclaim responsibility for any injury to people or property resulting from any ideas, methods, instructions or products referred to in the content.